Compressor Ring Studies for a 5 MW Spallation Neutron Source

G H Rees, Rutherford Appleton Laboratory, U.K.

Abstract

An outline design has been made of Compressor rings for a 5 MW spallation neutron source. Aspects of the design are discussed: magnet lattice, H^- injection, radiofrequency containment, extraction, beam loss collection, beam instability considerations and linac current levels.

1. Introduction

Three options have been considered for compressor rings fed from H^- linacs: 3 rings at 0.8 GeV and 1.7 MW each, 2 rings at 1.2 GeV and 2.5 MW each, or 1 ring at 2.4 GeV and 5 MW. The 3 or 2 ring option is favoured for the following reasons:

a. Cost.
b. Reliability (lose a ring and operation is still possible at $^2/_3$ or ½ intensity).
c. There is a longer linac to maintain for 2.4 GeV.
d. Debunching of the linac microbunches is slower at 2.4 GeV.
e. Momentum ramping for the linac is more difficult at 2.4 GeV.
f. The beam lines to the rings and target are more expensive at 2.4 GeV.
g. Beam loss collimation and collection is more difficult at 2.4 GeV.
h. More shielding is required for higher energy.
j. All rings have the same number of particles and, at the lower energies, more loss per ring is allowed due to the lower ring beam powers.
k. The ring has to be larger for 2.4 GeV, and since a linear lattice is preferred, there is a larger Q, and a larger chromatic Q spread.
l. Extraction is more difficult at 2.4 GeV as the ring aperture may not be reduced much with energy without increasing the transverse impedance.
m. H^- injection is more difficult at 2.4 GeV; there is a longer injection region, tighter tolerances, greater radiation damage to the foil, and more uncertainty about the metastable H° excited states.
n. The only target experience is at 0.8 GeV or less.

Against all these advantages for the lower energy rings must be weighed the difficulties associated with longer linac duty cycles, caused by the constraint of a given linac peak current. The effect of relaxing this constraint is discussed in the final section of the paper. Elsewhere, other ring features are described but with the 0.8 GeV case only considered.

2. Magnet Lattice

A lattice of 3 superperiods is chosen, as shown in Figure 2. There are separate regions of high dispersion for H^- injection and momentum collimation, and separate regions of zero dispersion for betatron collimation, extraction and radiofrequency systems. Each superperiod has 5 triplet cells, arranged with mirror symmetry about

FIG. 1

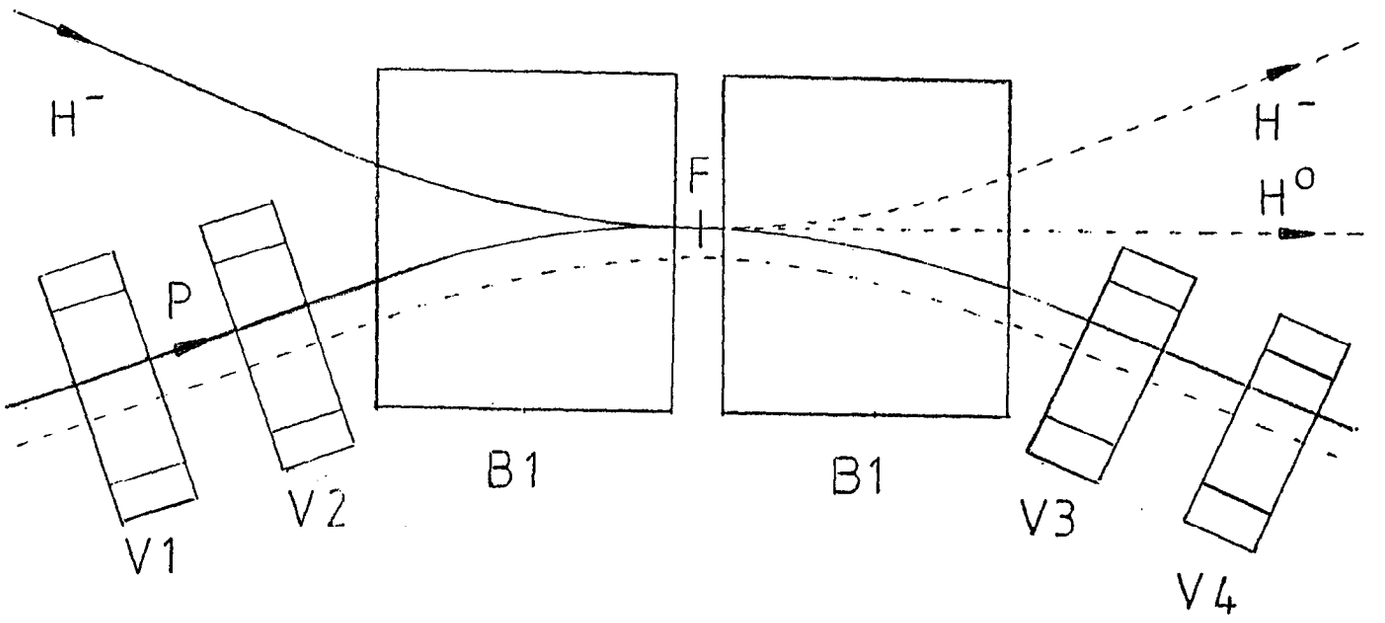

OPTIMISED H⁻ INJECTION

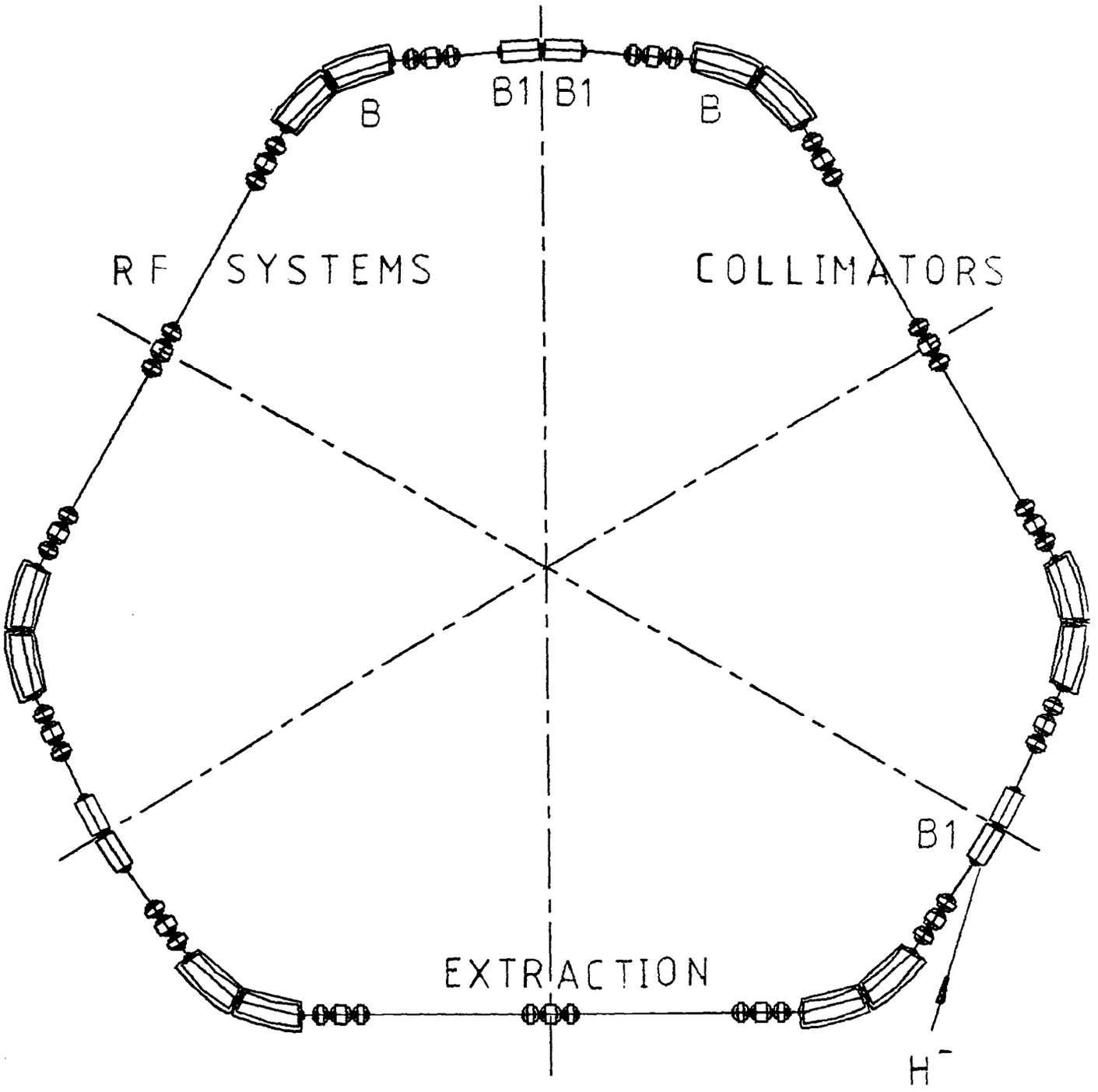

FIG. 2 LATTICE

the point where the parameters for the injection stripping foil are specified. Thus, only 3 of the 5 triplets are independent, and the 6 independent quadrupole gradients are adjusted to give $Q_x = 3.7$, $Q_y = 4.24$, β_y(peak) = 22.0 m, D_x(long straight) = 0, $\mu_x = \mu_y \geq 170°$ (long straight) and $D_x/\sqrt{\beta_x} = 2.7$ m $^{1/2}$ (foil). The last condition is required for optimised H^- injection, and the last but one for optimised beam loss collection. Rectangular bending magnets are used, of a relatively short length, and these contribute some vertical edge focusing. There are main bending magnets, B, and subsidiary units, B_1; the latter allow direct merging of the incoming H^- beam with the circulating protons. The operating point in the Q-diagram is located carefully with respect to fourth order betatron resonances excited by space charge; in this respect, the lattice is superior to one of superperiodicity 2. Lattice functions are shown in Figure 3.

3. H^- Injection

The H^- charge exchange system is the most critical item for the successful operation of the rings. The scheme proposed is shown in Figure 1, and occupies a region of approximately 9.1 m. There is a central stripping foil, the B1 lattice dipoles, and 4 identical dipoles to create a symmetrical vertical orbit bump. Use is made of a foil with 2 free, unsupported edges, and there is simultaneous 'painting' in the longitudinal and both transverse planes. Vertical painting is obtained by programming the vertical bump magnet system, and the horizontal and longitudinal painting by a ramping of the momentum of the input H^- beam. For the longitudinal painting, there is, in addition, a programming of the amplitudes of the radiofrequency containing fields. Optimised injection [1] is achieved by the use of the special foil, and by appropriate choices of the dispersion and betatron parameters in the injection region, together with mismatching for the injected beam. The proposed parameters reduce the average number of proton foil traversals during a 1000 turn injection interval to ~ 5. Beam loss in the rings is further minimised by chopping the H^- beam in the linac, with a duty cycle of ~ 60%, at the ring revolution frequency. A foil thickness of 275 μgm cm^{-2} is proposed, which strips ~ 98% of the 800 MeV H^- particles to protons, leaving most of the remainder as partially stripped H^o particles, in a range of quantum states. The fate of these H^o particles depends on their quantum state and the local value of the magnetic field (1.25 to 2.5 kG); the particles of low principal quantum number ($n < 5$) remain unstripped and pass out of the ring for external collection; the particles of $n \geq 7$ strip almost immediately in the magnetic fields at the foil, and are accepted as protons; there remain some $n = 5$ and 6 states, which strip after some delay, and so may be accepted, or lost, or pass into the beam halo. The choices of the field levels at the foil and B1 units are therefore very important. They are provisionally selected at 1.25 and 2.5 kG, respectively, which allows the foil stripped electrons to be intercepted in an adjacent collector, before they recirculate through the foil. An alternative arrangement is to replace the two, 2.5 kG, B_1 magnets by a long common unit with a uniform field of 1.25 kG, which is the optimum field level with respect to the $n = 5$ and 6 quantum state lifetimes. The foil is then at the centre position of this 1.25 kG magnet.

FIG. 3

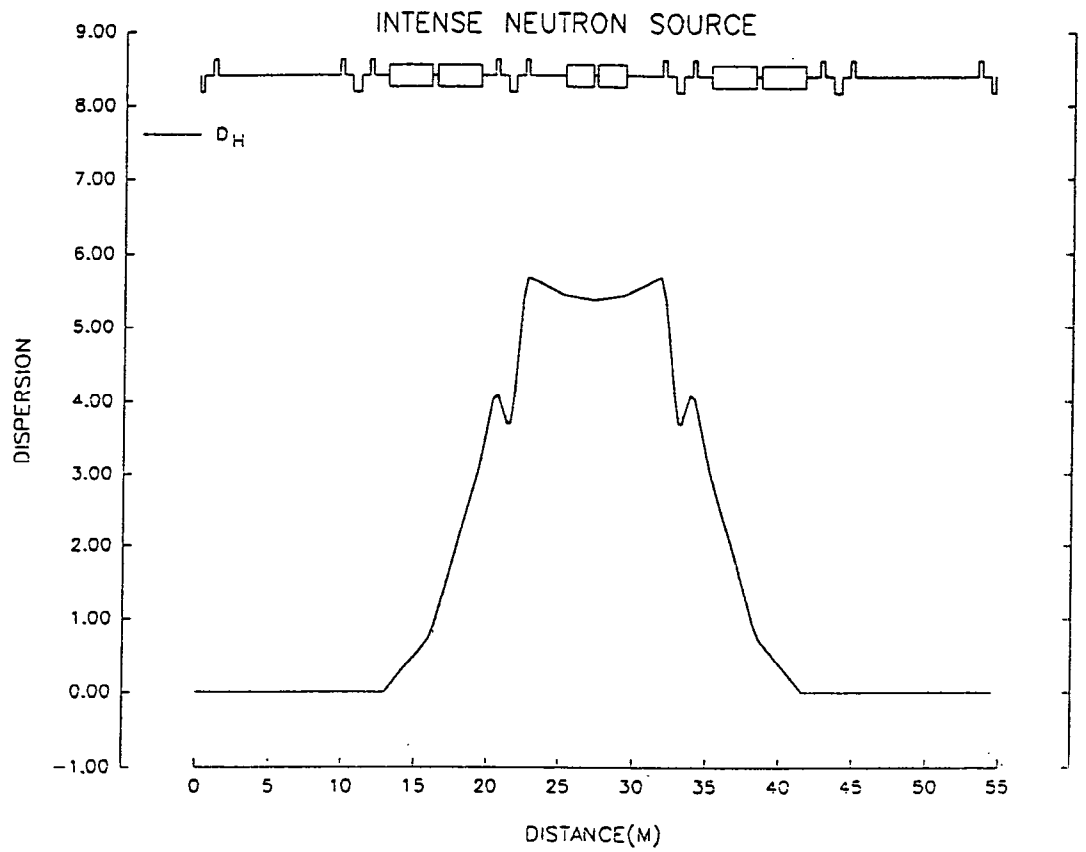
INTENSE NEUTRON SOURCE
D_H
DISPERSION
9.00
8.00
7.00
6.00
5.00
4.00
3.00
2.00
1.00
0.00
-1.00
0
5
10
15
20
25
30
35
40
45
50
55
DISTANCE(M)

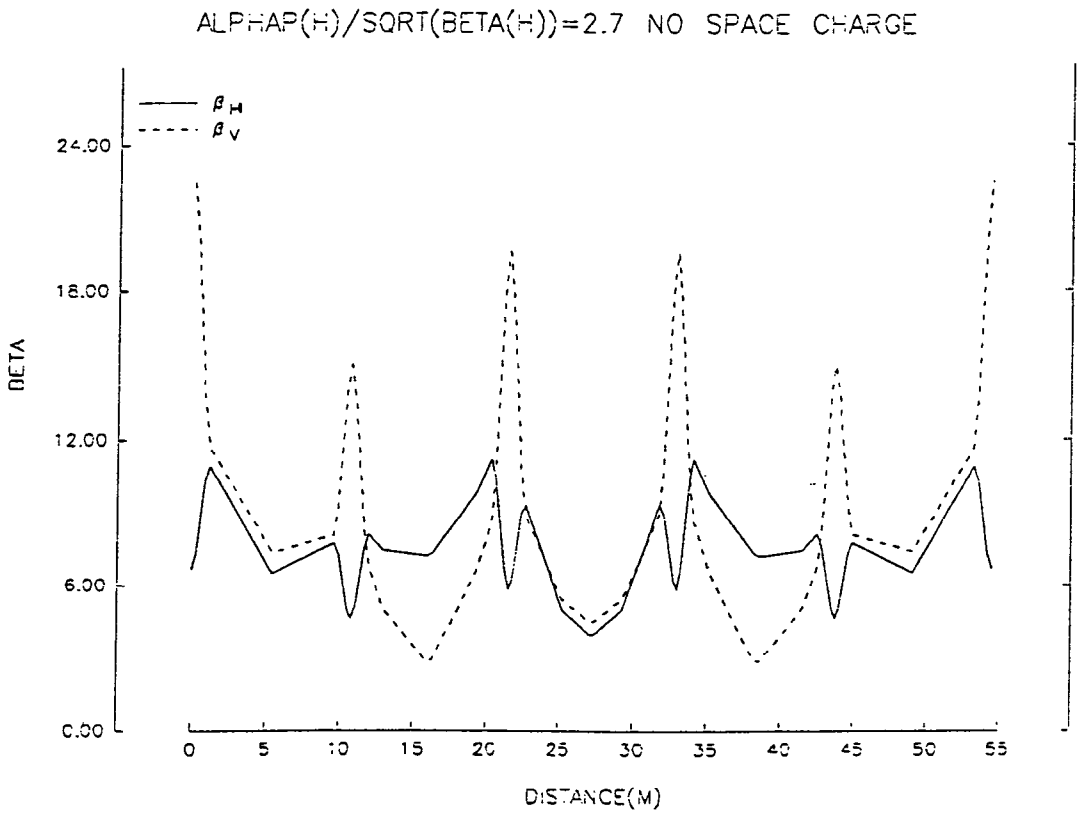
ALPHAP(H)/SQRT(BETA(H))=2.7 NO SPACE CHARGE
β_H
β_V
BETA
24.00
18.00
12.00
6.00
0.00
0
5
10
15
20
25
30
35
40
45
50
55
DISTANCE(M)

4. Radiofrequency Containment

The basic requirements for radiofrequency (rf) containment are set by the level of the longitudinal space charge forces in the rings. These forces may be reduced by ensuring that the stored beam has a reasonably uniform transverse density distribution, and by profiling the vacuum chamber envelope to follow a shape which is a fixed ratio to that of the adjacent beam envelope. The ratio cannot be too small or it will prevent the efficient action of a beam loss collection system; the ratio chosen is $4/\sqrt{5}$, leading to a longitudinal space charge parameter, g, of ~ 1.75. A low value of g is advantageous for it reduces the requirements for both the amplitude of the rf containing field and the amount of momentum ramping for the injected beam. The waveform of the rf containing field is non-sinusoidal, either rectangular for a barrier bucket, or that of a dual harmonic, h = 1 and h = 2 system. Assuming a phase extent of $\pm 0.691\ \pi$ in the rings, and longitudinal elliptical 2 - D density distributions, the required voltage amplitude/turn for these waveforms are ± 51.4 kV for the former, and ± 29.5 and ± 17.7 kV for the latter. The related fractional peak beam momentum spread is $\pm 5.5\ 10^{-3}$. The barrier bucket waveform may be generated approximately on an induction linac type cavity, or on a number (~ 5) of separate, harmonically related, resonant cavities. The latter is an extension of the arrangement proposed for the dual harmonic rf system. Initial ideas assume single, not twin, gapped cavities for reduced beam loading, and with ferrite and capacitive loading. A gap capacity of ~ 3500 pF leads to an R/Q value of ~ 30 Ω for the h = 1 system, and ceramic vacuum capacitors are available for gap voltages of ~ 15 kV. It may be sufficient to operate the cavities at a fixed tuning, at approximately half the detuning required for full reactive beam loading compensation. Alternatively, it may be possible to find a ferrite that is approximately optimally detuned by the proposed level of beam current. Control for the beam loading will also involve beam feed-forward or rf feedback systems.

5. Extraction

A fast extraction system is required, with beam loss less than 1 part in 10^4. This figure is achieved on the ISIS synchrotron, and a similar extraction system is proposed for the compressor rings. There are 3, push-pull, lumped kickers, with a total kicker rise time of ~ 180 ns, provided by 6 pulse generators per ring, at impedance, voltage and current levels of 8.33 Ω, 42 kV and 5000 A, respectively. A longitudinal ground plane threads each kicker, which is back terminated at the source, so that pulse forming networks are at an impedance level of 8.33/2 Ω. Induced volts for a centred beam in the kicker are estimated at < 5 V. More straight section space is available than in ISIS, so the extraction septum magnet design is simplified. An additional difference from ISIS is that there is no slow orbit bump, which has proved a complication for ISIS operation.

6. Beam Loss Collection

Activation and radiation damage of ring components may be reduced by localising the beam loss in betatron and momentum collectors. Such a system has proved very effective on the ISIS synchrotron, in particular the momentum collectors for untrapped 70 - 85 MeV protons. Collimation in the Compressor rings is more difficult because the beam energy is $\geq$ 800 MeV, and because growth in beam size is expected to be due more to transverse betatron than longitudinal synchrotron motion. Again, however, the use of collimators and collectors is proposed. Optimum criteria for betatron collection in a dispersion free region may be derived from a normalised betatron phase space diagram. It may be shown that if a primary collimator is located at a normalised transverse position, Z, and secondary collectors at positions Z_1 and - Z_1, after betatron phase shifts, μ_1 and μ_2, respectively, then optimum values are $\mu_1 = \cos^{-1}(Z/Z_1)$ and $\mu_2 = \cos^{-1}(-Z/Z_1)$, with Z_1 a few percent larger than Z. For high collection efficiency, it is necessary for the dispersion free region to extend over a μ range > 160°, and for there to be equal values of μ_2 in the 2 transverse phase planes. It is also advantageous to angle the upper or lower half of the collimator and collectors to improve the interception efficiencies. The optimised H^- injection process correlates large synchrotron oscillations with small horizontal betatron motion, so momentum collimation may be unnecessary. However, for protection, momentum collimators will be installed at a position where $D_x/\sqrt{\beta_x}$ is a maximum. It is proposed to use graphite collectors, where possible, to reduce the activation levels, with lengths of ~ 1 m to stop 800 MeV protons. The first collector is immediately downstream of the collimator, with the surface, Z_1, set back progressively as the distance downstream increases, with a maximum end value for Z_1 ~ 1.02 Z. A material of higher atomic number than graphite is preferred for the collimator, to reduce the amount of beam outscattered from its front surface.

7. Beam Instability Considerations

Bunched beam instabilities, only, need be considered. The maximum stored beam, N, is 2.6 10^{14} protons per ring, which is a factor 6 larger than has been achieved on ISIS at 70 MeV, where there has been no sign of a bunched or unbunched electron-proton instability. The momentum spread of the ISIS beam at 70 MeV is $\pm$ 2 10^{-3}, a factor of ~ 3 smaller than that proposed for the 800 MeV compressor rings. At LANL, however, an e-p instability has been observed on the Proton Storage Ring, at intensities comparable to those of ISIS. The differences between ISIS and the PSR include for ISIS; smoother chamber transitions, larger transverse emittances, a somewhat larger circumference, and collection of the foil stripped electrons. All these safeguards are proposed for the Compressor. For bunched beam longitudinal stability, it is advantageous to profile the vacuum envelope to reduce the g parameter, and to improve the transverse distributions by the H^- painting process, as mentioned previously. Since the injection interval corresponds to ~ 1.5 synchrotron periods, it is considered unlikely that a coherent longitudinal or a coherent head-tail transverse mode has time to develop. The latter would have to be a very high order mode because it is planned to operate with the natural value of the ring chromaticities.

8. Linac Current Levels

The maximum injection duty cycle of each compressor ring is limited to ~ $3^1/_3$%, so if the rings for the 800 MeV option are fed sequentially, the total linac duty cycle is 10%. The average linac beam current during the pulse is then 62.5 mA and the peak value, due to the chopping at the ring revolution frequency, is 105 mA. A reference H^- linac may be defined for this current, using funneling at low energy to reduce the ion source requirements. Such a linac may be room temperature (RT) or superconducting (SC). The optimum ratio for the total rf power to the beam power, during the beam pulse, may be expressed as $1 + (R_b/R_c)$, where R_b and R_c are transit time corrected beam and cavity shunt resistances, respectively, with $R_b = V/(I_b \cos \phi_s)$ and $\phi_s \sim -25°$. For a SC linac, the total rf power to provide the beam pulse is thus ~ 5 MW, and for the proposed, 440 m, 700 MHz, RT linac ~ 10 MW. In addition, the klystrons, circulators and loads must introduce additional power during the on and off pulsing of the cavity fields. For the suggested SC linac, this power is considerable, as the parameters considered are cavity frequencies of 350 MHz and loaded cavity Q-values of 10^6, corresponding to cavity filling times of 1 ms, and total rise or fall times for the cavity fields of ~ 4 ms. The filling time is reduced by an order of magnitude by raising the frequency to 700 MHz and lowering the loaded Q to 2 10^5; even so, this is still an order of magnitude larger than for the RT linac. Finally, the effect of relaxing the peak current constraint for the RT linac may be considered, hence reducing R_b. In one scheme envisaged, the duty cycle of the chopping may be changed, and the linac current increased to ~ 200 mA, eg by adding a further stage of funneling and using special high duty cycle chopping at low energy, correlated with 3-way switching at high energy for repeated sequential filling of the 3 rings at a 60% duty cycle, every second turn. In this mode, the linac duty cycle is reduced to $3^1/_3$%. The proposed scheme is of interest because of the potential cost saving, but for it to be feasible, higher peak power klystrons have to be developed, and also a low beam loss, high energy beam chopper. Peak currents in the main linac are approximately doubled. Some increase in the cavity fields may also be considered to reduce the length of the linac.

Reference

[1] G H Rees and H Zhang, RAL design notes for the ESS, EPNS/RAL/A2-91 and A4-92, 1991-92.